

Slow magnetic dynamics in the K3M3IIM2IIIF15 multiferroic system

Pajić, Damir; Jagličić, Zvonko; Trontelj, Zvonko

Source / Izvornik: **Journal of Applied Physics, 2012, 112**

Journal article, Published version

Rad u časopisu, Objavljena verzija rada (izdavačev PDF)

<https://doi.org/10.1063/1.4757006>

Permanent link / Trajna poveznica: <https://urn.nsk.hr/urn:nbn:hr:217:462881>

Rights / Prava: [In copyright](#) / [Zaštićeno autorskim pravom.](#)

Download date / Datum preuzimanja: **2025-03-22**



Repository / Repozitorij:

[Repository of the Faculty of Science - University of Zagreb](#)



Slow magnetic dynamics in the K₃M₃IIM₂IIIF₁₅ multiferroic system

Damir Pajić, Zvonko Jagličić, and Zvonko Trontelj

Citation: *J. Appl. Phys.* **112**, 073908 (2012); doi: 10.1063/1.4757006

View online: <http://dx.doi.org/10.1063/1.4757006>

View Table of Contents: <http://jap.aip.org/resource/1/JAPIAU/v112/i7>

Published by the [American Institute of Physics](#).

Related Articles

Exchange bias and memory effect in double perovskite Sr₂FeCoO₆

Appl. Phys. Lett. **101**, 142401 (2012)

Spin dynamics of S=1/2 Heisenberg chains with a staggered transverse field: electron spin resonance studies (Review Article)

Low Temp. Phys. **38**, 819 (2012)

Spin-wave excitations induced by spin current through a magnetic point contact with a confined domain wall

Appl. Phys. Lett. **101**, 092405 (2012)

Spin wave localization and softening in rod-shaped magnonic crystals with different terminations

J. Appl. Phys. **112**, 033911 (2012)

Direct imaging of spin relaxation in stepped α -Fe₂O₃/Ni₈₁Fe₁₉ bilayers using x-ray photoemission electron microscopy

Appl. Phys. Lett. **101**, 052403 (2012)

Additional information on J. Appl. Phys.

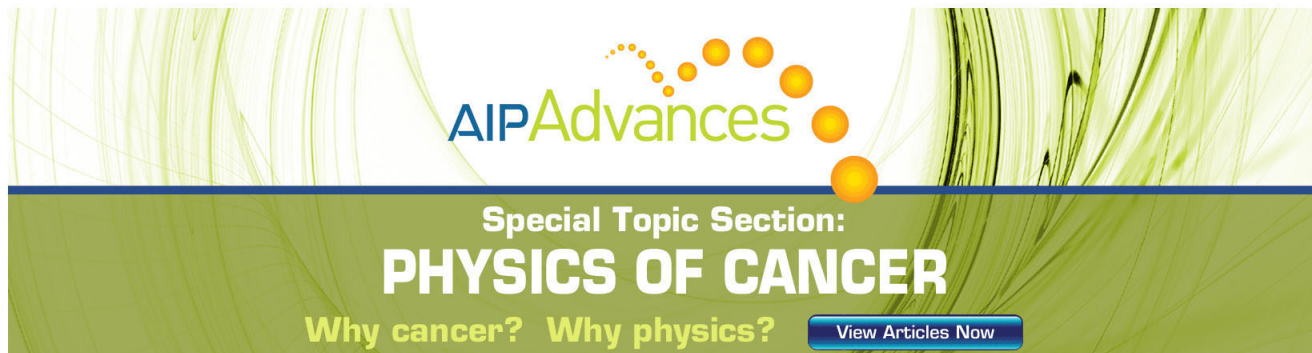
Journal Homepage: <http://jap.aip.org/>

Journal Information: http://jap.aip.org/about/about_the_journal

Top downloads: http://jap.aip.org/features/most_downloaded

Information for Authors: <http://jap.aip.org/authors>

ADVERTISEMENT

The advertisement features a green background with abstract, flowing, wavy lines in a lighter green shade. At the top, the text 'AIPAdvances' is displayed in a green, sans-serif font. Below this, the text 'Special Topic Section:' is written in a smaller, white, sans-serif font. The main title 'PHYSICS OF CANCER' is prominently displayed in a large, bold, white, sans-serif font. Below the title, the text 'Why cancer? Why physics?' is written in a smaller, white, sans-serif font. In the bottom right corner, there is a blue button with the text 'View Articles Now' in white.

Slow magnetic dynamics in the $K_3M_3^{II}M_2^{III}F_{15}$ multiferroic system

Damir Pajić,^{1,2} Zvonko Jagličić,^{1,3} and Zvonko Trontelj^{1,a)}

¹*Institute of Mathematics, Physics and Mechanics, Jadranska 19, 1000 Ljubljana, Slovenia*

²*Department of Physics, Faculty of Science, University of Zagreb, Bijenička c. 32, 10000 Zagreb, Croatia*

³*Faculty of Civil and Geodetic Engineering, University of Ljubljana, Jamova c. 2, 1000 Ljubljana, Slovenia*

(Received 13 July 2012; accepted 30 August 2012; published online 2 October 2012)

$K_3Fe_5F_{15}$ is a multiferroic material belonging to the $K_3M_3^{II}M_2^{III}F_{15}$ family. Zero-field cooled and field cooled magnetization measured as a function of temperature demonstrate magnetic transition in $K_3Fe_5F_{15}$, $K_3Fe_3Cr_2F_{15}$, and $K_3Cu_3Fe_2F_{15}$. Complementary to this, the magnetic behavior below the magnetic transition was studied via magnetic relaxation at different temperatures after switching magnetic field from H to $-H$. A slow change of magnetization on the hours time scale was observed and it was best described by a logarithmic time dependence for all three compounds over a broad temperature and field range. It follows that a distribution of magnetic moments over anisotropy barriers, which block the magnetic moments against reorientation, is present. We introduced a model of thermal activation of the magnetic moments of regions distributed over the barriers to describe the temperature and field dependence of the relaxation parameters. The dimensions of these magnetic regions were estimated to be of nanometer size. © 2012 American Institute of Physics. [<http://dx.doi.org/10.1063/1.4757006>]

I. INTRODUCTION

Magneto-electric materials with (anti)ferromagnetic (FM, AFM) and ferroelectric (FE) properties are of great interest in solid state physics due to possible coupling of magnetic and electric orders.^{1–3} The possibility of influencing one order parameter by a change of another is opening new perspectives for applications in spintronics, memory devices, novel sensors, etc.^{4–8}

In the search for novel multiferroic systems, the vast majority of materials obtained belong to the class of oxides, with $BiFeO_3$ being the best known.⁴ The perovskite, or tetragonal tungsten bronze (TTB) structure is often present, as in $Ba_2NaNb_5O_{15}$ and its extensions.⁹ By substituting oxygen with fluorine¹⁰ and including lower valence transition metals,¹¹ the route to new multiferroic materials is open.^{12,13} One of them is the ferroelastic compound $K_3Fe_5F_{15}$ with a ferroelastic-ferroelectric transition at 490 K¹⁴ and a second order magnetic phase transition at 122 K.¹⁵ Further studies showed the appearance of weak ferromagnetism below 122 K.¹⁶ In $K_3Fe_5F_{15}$, the substitution of Fe^{3+} ions by Cr^{3+} , and of Fe^{2+} by Cu^{2+} is allowed.¹⁷ Initial studies on $K_3Cu_3Fe_2F_{15}$ demonstrated antiferromagnetic interactions and partial ordering of the system in coexistence with regions without magnetic order.¹⁸ The obtained fluoride family could be represented by the general formula $K_3M_3^{II}M_2^{III}F_{15}$ having the orthorhombically deformed TTB structure with the $Pba2$ space group.¹⁹ The magnetic properties of $K_3M_3^{II}M_2^{III}F_{15}$ have not been fully investigated, and to our knowledge only the multiferroic phase diagram of $K_{0.6}Fe_{0.6}^{II}Fe_{0.4}^{III}F_3$ was constructed.²⁰

The compounds $K_3Fe_5F_{15}$, $K_3Fe_3Cr_2F_{15}$, and $K_3Cu_3Fe_2F_{15}$ were the objects of this research, with the aim of

investigating their slow magnetic relaxation and determining the size of magnetically ordered volumes.

Some partial static magnetic investigations have been performed,^{15–18} and here we completed them with the missing temperature dependencies of magnetization for a broad interval of magnetic fields. So far, the investigation of relaxation and dynamics was limited to ^{39}K NMR and EPR within their specific time windows.²¹ Here, we present in details the study of slow magnetic dynamics in the DC region, including the dependence of relaxation parameters on field and temperature, for all three compounds.

II. EXPERIMENTAL

Polycrystalline $K_3Fe_5F_{15}$ was prepared from stoichiometric quantities of KF , FeF_2 , and FeF_3 at 1000 K under dry argon in a sealed gold tube.¹⁶ The reaction mixture was left in an oven for 15 days to obtain polycrystalline samples. $K_3Fe_3Cr_2F_{15}$ was synthesized using a slightly modified method where the solid state reaction of KF , FeF_2 , and CrF_3 in 3:3:2 molar ratio proceeded at 1000 K in a gold tube over 14 days.¹⁷ Similarly, $K_3Cu_3Fe_2F_{15}$ was prepared from KF , CuF_2 , and FeF_3 .¹⁸

The crystal structures of all prepared compounds were checked by x-ray diffraction to be in accordance with the published data for $K_3Fe_5F_{15}$.¹⁹ We confirmed that $K_3Fe_3Cr_2F_{15}$ and $K_3Cu_3Fe_2F_{15}$ are isostructural at room temperature with $K_3Fe_5F_{15}$.^{17,18,22}

Magnetic measurements were performed using a commercial QD MPMS-XL-5 SQUID magnetometer. The relaxation of magnetization after a change of magnetic field at constant temperature was measured thoroughly as follows: The sample was cooled down to the desired temperature from above the magnetic transitions in a magnetic field H , and after reversing the magnetic field from H to $-H$ the time dependence of magnetization was measured at the constant

^{a)}Electronic mail: zvonko.trontelj@fmf.uni-lj.si.

temperature. This relaxation was measured in magnetic field spanning at least three or four orders of magnitude and a broad temperature range for each sample. In addition, the so-called thermoremanent magnetization, $M_{TRM}(T)$, was measured as follows: The sample was cooled down to the lowest temperature (2 K) in a magnetic field H from above the magnetic transition, and after reversing the magnetic field from H to $-H$ the measurement of magnetization was performed during heating, using the constant heating rate of 1 K/min for $K_3Fe_5F_{15}$ and $K_3Fe_3Cr_2F_{15}$ and 0.2 K/min for $K_3Cu_3Fe_2F_{15}$.

As a complement to our previous magnetic measurements,^{16–18} the temperature dependence of magnetization $M(T)$ during heating in different fields, after zero field cooling (ZFC) and after field cooling (FC), as well as the magnetization vs. field dependences $M(H)$, was measured.

The temperature stability during the relaxation measurement was within several mK at low temperatures and within 0.1 K at high temperatures. The relative error in all static and time dependent magnetic measurements was much less than 0.1%.

III. RESULTS

A. Magnetic relaxation

The complete $M(T)$ dependences for different H in the relevant temperature intervals for $K_3Fe_5F_{15}$, $K_3Fe_3Cr_2F_{15}$, and $K_3Cu_3Fe_2F_{15}$ polycrystals are shown in Fig. 1, where M/H is plotted on the vertical axis.

Although these three systems show some similarities concerning the irreversibility expressed through the ZFC-FC splitting, the obvious differences in $M(T)$ curves between $K_3Fe_5F_{15}$, $K_3Fe_3Cr_2F_{15}$, and $K_3Cu_3Fe_2F_{15}$ still require an explanation regarding the magnetic ordering.

Some of the relaxations of magnetization are shown in Fig. 2 for all three compounds. All of the data recorded for 1 h exhibited a logarithmic $M(t)$ dependence for each temperature and field where the ZFC-FC splitting appears. Therefore, the fitting function

$$M(t) = M_0 - S \cdot \ln(t - t_0) \quad (1)$$

was used (with time in seconds), whose agreement with the measured data is shown in Fig. 2. In $K_3Fe_5F_{15}$, the relaxation is logarithmic at temperatures below 122 K, even in a field of 10 kOe, showing strong interaction of magnetic moments in $K_3Fe_5F_{15}$. The relaxation of magnetization of $K_3Fe_3Cr_2F_{15}$ is logarithmic over the four orders of magnitude of the magnetic fields explored and for temperatures up to the ZFC-FC splitting temperature (maximally 40 K). $K_3Cu_3Fe_2F_{15}$ exhibits slow logarithmic relaxation only below 30 K and in an applied magnetic field up to 100 Oe. The absence of measurable relaxation for 1 kOe field or larger could be anticipated from the disappearance of ZFC-FC splitting in this field.

M_0 in Eq. (1) is the starting magnetization from which it begins to relax slowly. The change of magnetization from the value determined by cooling in field H , toward the new value following the reversal of the field to $-H$, happens in a short time until M_0 is reached. This part of the relaxation is not measurable by our instrument, as it happens mainly

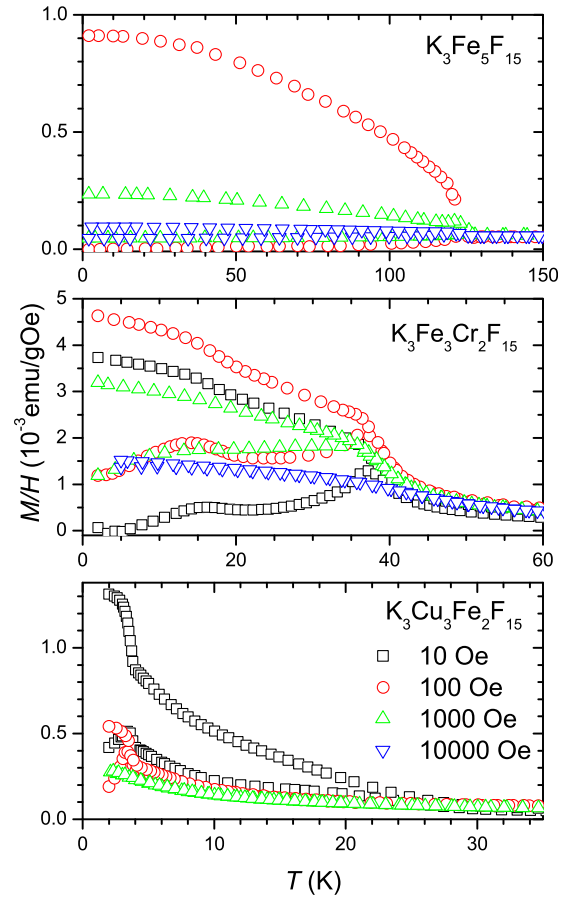


FIG. 1. Measured temperature dependence of ZFC-FC magnetization divided by field for three compounds and different magnetic fields. The same legend applies for all three graphs.

during recharging of the magnet. These indeterminable starting changes are described by introducing the t_0 parameter in Eq. (1). Rather similar fitted t_0 values were obtained for all samples, being between 30 and 60 s for a smaller change of field and between 40 and 80 s for a larger change of field. The standard deviation of t_0 was of the order of magnitude of 1 s. S in Eq. (1) reflects the rate of change of magnetization over time on a logarithmic scale.

B. Logarithmic relaxation rate S

The temperature dependence of the logarithmic relaxation rate S for different magnetic fields, obtained from fitting Eq. (1) to the $M(t)$ measurements, is shown in Fig. 3 for all three compounds. The reproducibility of the data was confirmed and the relative error of S is 0.1%–2%.

For $K_3Fe_5F_{15}$, two maxima occurred on $S(T)$ in the lowest field of 100 Oe, at 90 K and 120 K. With increase of field to 1 kOe, a shift of the maxima to lower temperatures appeared: one is at 30 K and the other between 110 and 115 K. In the highest field of 10 kOe, a broadening of the $S(T)$ maxima appeared, leading to considerable smearing and overlapping.

For $K_3Fe_3Cr_2F_{15}$, two maxima in $S(T)$ appeared for lower fields: at 10 K and 30 K for 10 Oe, and at 7 K and 25 K for 100 Oe. Only one clear maximum appeared at 10 K for

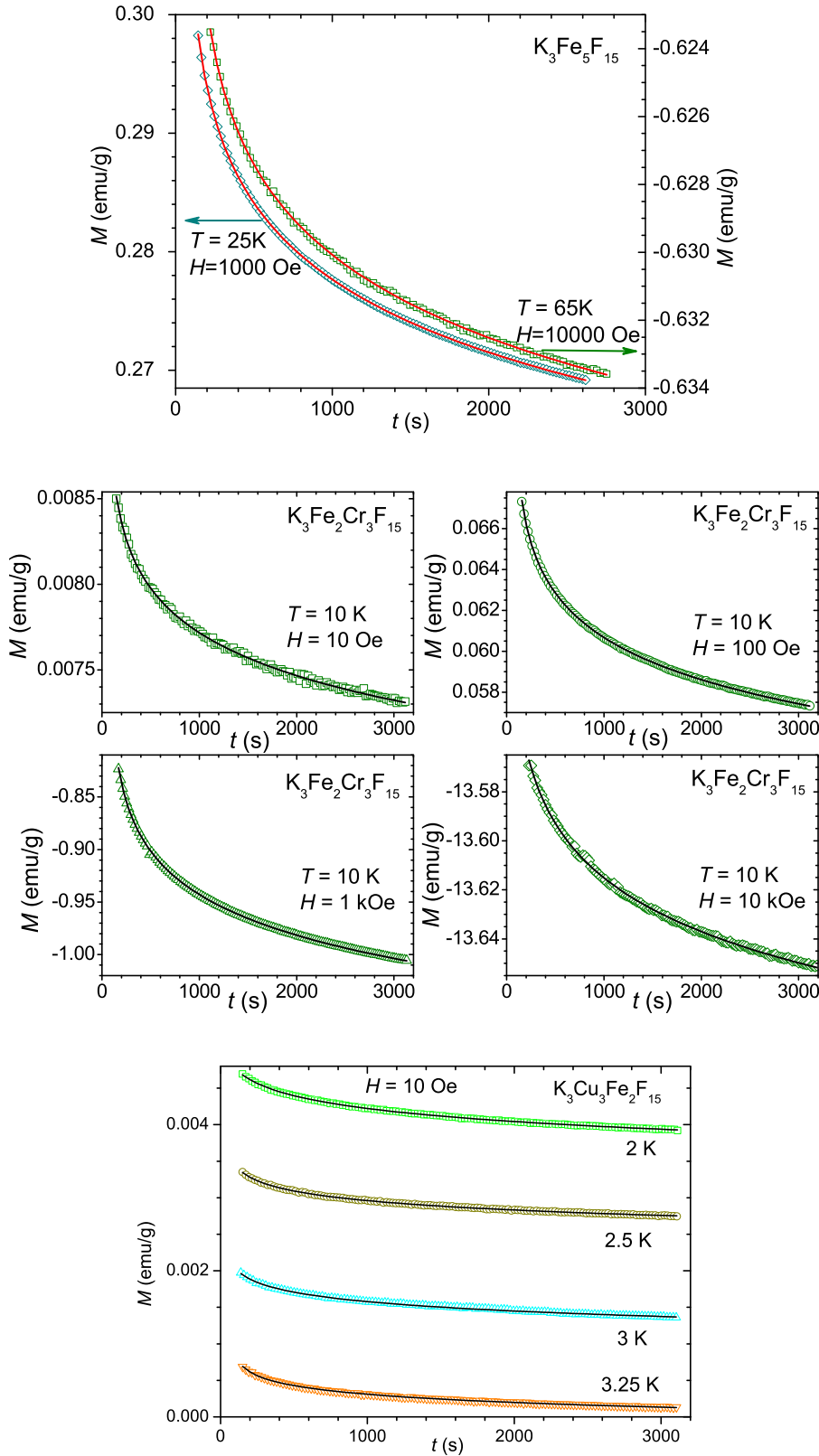


FIG. 2. Some typical magnetization relaxation curves of $\text{K}_3\text{Fe}_3\text{F}_{15}$ (upper panel), $\text{K}_3\text{Fe}_2\text{Cr}_3\text{F}_{15}$ (middle 4 panels), and $\text{K}_3\text{Cu}_3\text{Fe}_2\text{F}_{15}$ (lower panel) after different magnetic field reversals from H to $-H$. Lines are the logarithmic fitting curves defined by Eq. (1).

1 kOe, and the shoulder at 4 K indicates an overlapped maximum. No maxima were observed for 10 kOe down to 3 K.

For $\text{K}_3\text{Cu}_3\text{Fe}_2\text{F}_{15}$, $S(T)$ was determined in 10 Oe and 100 Oe only, while 1 kOe reversed the magnetization instantaneously without measurable relaxation. In this compound also the two maxima could be anticipated for lowest fields, but all what we can see in Fig. 3 is the broad maximum at

10 Oe field, almost a knee, centered at 15 K and a strong rise in the $S(T)$ at 6 K.

C. Starting magnetization M_0 and thermoremanent magnetization M_{TRM}

The behavior of the starting magnetization, $M_0(T)$, of all three compounds is shown in Fig. 4. The fitting parameter

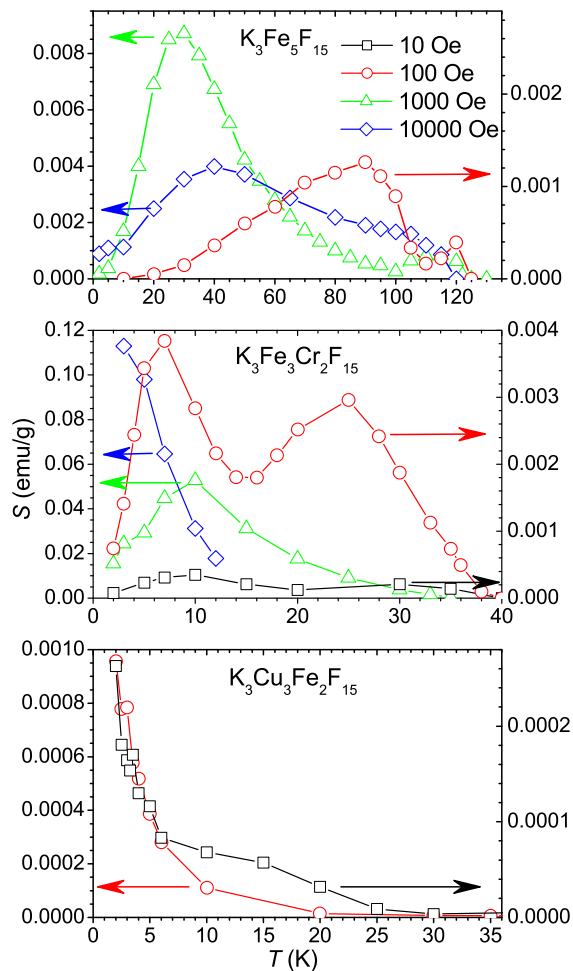


FIG. 3. Temperature dependence of logarithmic relaxation rate S for three compounds determined from the relaxation of magnetization measured after a change of magnetic field from H to $-H$ for different H . Lines are eye-guides only. The same legend applies for all three graphs.

M_0 for all the relaxation data sets was within 0.05%–0.5% relative standard error.

For $K_3Fe_5F_{15}$, there are two characteristic steepest decreases in $M_0(T)$ observed for 1 kOe and 10 kOe: for 1 kOe at 30 K and 115 K, and for 10 kOe at slightly lower temperatures. These temperatures indicate the onset of magnetic moment blocking by the two different groups of energy barriers in the system. A higher field was capable of turning the magnetic moments at somewhat lower temperature, and a lower field required higher temperatures to reverse them. As seen from Fig. 4, a field of 100 Oe could not reverse the magnetization into the new field direction, meaning that the majority of magnetic moments stayed blocked in direction of the cooling field. The assumption of two groups of magnetic moments having different reversal barriers, based on the $M_0(T)$ results, is consistent with the behavior of both $S(T)$ and ZFC $M(T)$.

Comparing the $M_0(T)$ plots for $K_3Fe_3Cr_2F_{15}$ in Fig. 4, we can see the existence of two minima for the lower field of 100 Oe (at 16 K and 37 K) and one minimum for the higher field of 1 kOe (at 32 K). This is reminiscent of the maxima on the ZFC curves in Fig. 1 for corresponding fields. The positions of the maxima on the ZFC $M(T)$ curves and the

minima on the $M_0(T)$ curves for the 10 Oe field are at the same values as for 100 Oe, indicating the persistence of barriers under the application of a relatively small magnetic field.

The existence of two groups of magnetic moments in $K_3Cu_3Fe_2F_{15}$ is implied by the $M_0(T)$ curves shown in Fig. 4 for the 10 Oe and 100 Oe relaxation measurements. The stronger field reverses the magnetic moments of both groups immediately, whereas the second group obviously becomes resolvable with the lower field at higher temperature through the steepest change of M_0 at around 15 K. The corresponding higher temperature bump around 15 K can also be observed on the $S(T)$ dependence for 10 Oe in Fig. 3.

Measured $M_{TRM}(T)$ dependences are shown in Fig. 4 by the full lines. For $K_3Fe_5F_{15}$, the field of 100 Oe is not strong enough to reverse the magnetization up to temperatures very near to T_N . Even the measurements in 1 kOe point to the high thermal energy needed to reverse the magnetic moments. Above 53 K, the magnetic moments continued to reverse up to 100 K, and above 100 K thermal influences started to decrease the value of the magnetization. Reversal of the major part of the magnetization of $K_3Fe_5F_{15}$ induced by a 10 kOe field occurred immediately and was completed at 10 K. However, for all fields there was a clear bumpy feature around 120 K, showing that the phase transition at 122 K is field-independent.

The M_{TRM} curve of $K_3Fe_3Cr_2F_{15}$ measured in a 1 kOe field showed that on increasing the temperature from the lowest up to 6 K there was no switching, indicating a well locked magnetic state under these conditions. Above 15 K (for the same 1 kOe measurement), there was an observable effect of additional excitation of magnetization that belongs to the magnetic regions with higher barriers. More indicative is the 100 Oe $M_{TRM}(T)$ curve with a well developed knee-shaped broad inflection region around the somewhat higher temperature of 20 K. However, the strongest field of 10 kOe changed the magnetization very near to the maximum negative value already at low temperature, and only the minority of still unrelaxed magnetic regions contributed to the temporal change of magnetization.

Similar phenomenon is present in $K_3Cu_3Fe_2F_{15}$, but occurs within an order of magnitude smaller magnetic field than in $K_3Fe_3Cr_2F_{15}$, due to much lower energy barriers. For M_{TRM} measurement in a 10 Oe field, the $K_3Cu_3Fe_2F_{15}$ system remained magnetized in a positive direction at the lowest temperature (2 K), and started to reverse its magnetization very quickly above 3 K (Fig. 4). After thermal decrease of magnetization up to 10 K, another magnetic component was excited up to 20 K. A magnetic field of 100 Oe reversed this part of the system immediately and swept out the bump observed at 20 K in the smaller field, whereas the low temperature peak still remained prominent spreading between 3 K and 4 K. Therefore, the higher temperature bump corresponds to those magnetic regions which were completely turned over by the 100 Oe field. The system was completely reversed by a field of 1 kOe and showed only a thermal decrease of magnetization value.

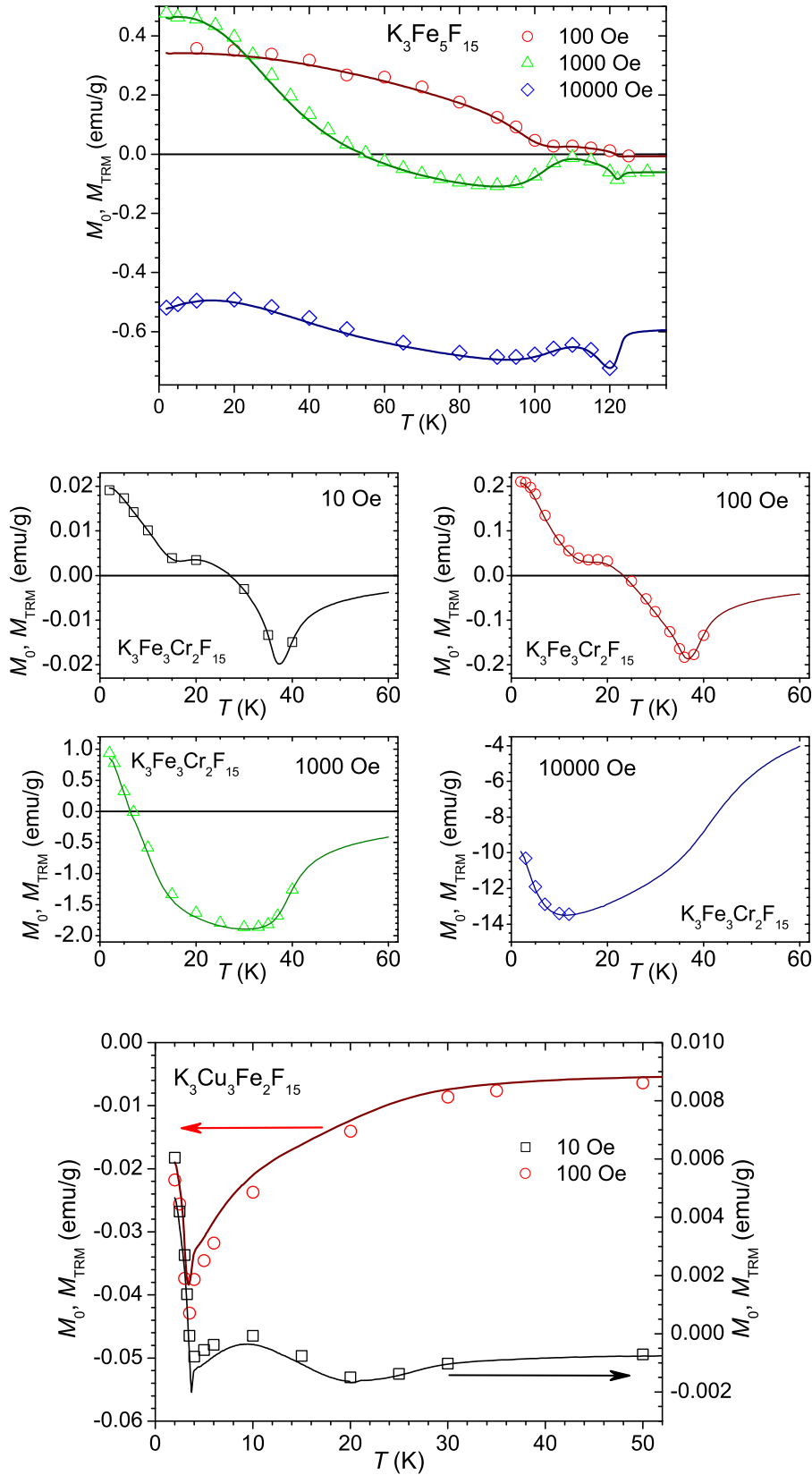


FIG. 4. Temperature dependence of starting magnetization $M_0(T)$ (symbols) for magnetic relaxations of $K_3Fe_5F_{15}$ (upper panel), $K_3Fe_3Cr_2F_{15}$ (middle 4 panels), and $K_3Cu_3Fe_2F_{15}$ (lower panel) in different fields. Lines are the measured $M_{TRM}(T)$ curves for corresponding fields.

IV. DISCUSSION

A. Logarithmic relaxation

The logarithmic relaxation of the system, $M(t) \propto \ln t$, appears when there is a distribution of magnetic moments over the anisotropy energy barriers present.²³ Recently, the anisotropy

of $K_3Fe_5F_{15}$ monocrystal was observed,²⁴ providing background for the anisotropy energy barriers in our case. The presence of logarithmic relaxation in our samples shows that for every temperature there is a large enough contribution to magnetization from the regions having activation energies suitable for exhibiting relaxation around this specific temperature.

In Fig. 3, the same generic behavior of $S(T)$ is seen in every compound, with two well localized maxima present for lower fields. These maxima reveal the existence of two groups of magnetic moments with different activation energies, well separated within the distribution. The shift of maxima toward lower temperatures with increasing field is due to the influence of the magnetic field on barrier reduction, allowing the activation of magnetic moments at lower temperatures. A further increase of field removes the lower temperature maximum, and eventually moves the higher maximum to experimentally inaccessible low temperatures.

The logarithmic relaxation of magnetization with time was previously observed in different nanostructured magnetic ensembles with magnetic moments distributed over the barriers.^{25–29} Though the logarithmic time relaxation generically occurs in glass forming systems,^{30,31} our results therefore give a hint that the relaxing entities could be the locally ordered magnetic regions. Temperature dependences of the magnetization and logarithmic relaxation rate considered together give a more complete picture of the behavior of magnetic moments of the regions and support their activation.

B. Thermal activation and diverse T-H scales

A striking feature is the same behavior of the logarithmic relaxation rate $S(T)$, ZFC $M(T)$ magnetization curve, starting magnetization $M_0(T)$ and thermoremanent magnetization $M_{TRM}(T)$. This is most obviously expressed for $K_3Fe_3Cr_2F_{15}$ if Figures 1, 3, and 4 are compared, and this kind of matching is valid for $K_3Fe_5F_{15}$ and $K_3Cu_3Fe_2F_{15}$ too.

More generally, $M_{TRM}(T)$ and $M_0(T)$ behaviors are correlated with $S(T)$ for all applied fields. The change of magnetization in two main steps on the M_{TRM} curve means that there is one group of magnetic moments with smaller barriers traversed at lower temperatures and a second well separated group with a higher temperature over-barrier crossing. The two component model is consistent with the $S(T)$ dependence, indicating that the change of magnetization during heating is strongly related to the relaxation mechanism. This relation is additionally proved by very good overlap of the M_0 starting magnetization parameter with the measured M_{TRM} curves (Fig. 4). However, for all M_{TRM} curves, the stepwise changes are gradual but not sharp, indicating a broad distribution of energies that should be crossed by the magnetic moments to relax the magnetization of the systems.

ZFC-FC irreversibility in the lowest measured field appears below 122 K, 40 K, and 26 K, for $K_3Fe_5F_{15}$, $K_3Fe_3Cr_2F_{15}$, and $K_3Cu_3Fe_2F_{15}$, respectively, reflecting the general magnetic transition behavior. The persistence of a ZFC-FC splitting temperature under application of magnetic field also develops in this sequence. In $K_3Fe_5F_{15}$, the splitting temperature does not move as the measuring field increases. This behavior indicates the presence of long range order. Convincing evidence for weak ferromagnetic order is found if the $M(T)$ curves are compared with the ZFC-FC curves of $LaMnO_3$, which was found to be a weak ferromagnet originating from canted antiferromagnetism.³² Presence of the long range order in $K_3Fe_5F_{15}$ was also argued from the frequency independence of the sharp AC susceptibility peak at 122 K.¹⁶

In $K_3Fe_3Cr_2F_{15}$ for a 100 Oe field, the ZFC $M(T)$ curve exhibits two maxima, around 36 K and 14 K. These peaks, also present in the AC susceptibility curve, were previously found to shift with frequency in a manner suggesting a short range ordered state.¹⁷ However, the lower temperature peak is more frequency dependent, indicating superparamagnetic fluctuations are likelier than collective freezing. Here, this is further supported by the pronounced movement of the lower temperature ZFC $M(T)$ peak (or knee for higher fields) with increasing magnetic field, while the higher temperature peak moves only slightly.

In $K_3Cu_3Fe_2F_{15}$, a considerable ZFC-FC difference appears below a temperature of 4 K in 100 Oe, while a small difference survives up to much higher temperatures. The rather sharp peak in magnetization $M(T)$ of $K_3Cu_3Fe_2F_{15}$ around 4 K and the bumpy feature above the peak observable for the low field measurement (10 Oe) conform with the temperature behavior of AC susceptibility.³³

These and previous results^{15,16} support the coexistence of regions with long range magnetic ordering in $K_3Fe_5F_{15}$ below $T_N = 122$ K and finite magnetic regions exhibiting time relaxation. In $K_3Fe_3Cr_2F_{15}$ and $K_3Cu_3Fe_2F_{15}$, the short range ordering is even more likely, as indicated by movement of the ZFC-FC splitting point toward lower temperature with increase of magnetic field, and even by the disappearance of splitting in the strongest fields. Additionally, for $K_3Fe_3Cr_2F_{15}$, short range order was proposed from AC susceptibility measurements¹⁷ and for $K_3Cu_3Fe_2F_{15}$ from EPR experiments.¹⁸ From the splitting temperatures, it can be concluded that the ratio of the energy barriers that block the magnetic regions against reorientation for $K_3Fe_3Cr_2F_{15}$ and $K_3Cu_3Fe_2F_{15}$ is around 10 when the 100 Oe measurements are compared. Interestingly, the fields needed to destroy the barriers and irreversibility are also around the same ratio of 10. Regarding this kind of irreversibility, the behavior of $K_3Fe_3Cr_2F_{15}$ is energetically somewhere between $K_3Fe_5F_{15}$ and $K_3Cu_3Fe_2F_{15}$. This ratio is supported by the thermoremanent magnetization $M_{TRM}(T)$ behavior, which shows more details about the influence of increasing thermal energy on the relaxation processes. Comparing plots in Fig. 4, the relation between barrier heights is seen, as well as the two component nature of magnetization revealed by two stepwise changes. Additional confirmation of different energy barriers comes from positions of the maxima in $S(T)$ dependences (Fig. 3).

Experimental consistency between the ZFC-FC $M(T)$ curves, M_0 parameter, $S(T)$ behavior, and $M_{TRM}(T)$ is clearly described by the model of consecutive activation of magnetic region's moments over the barriers. It follows that the macroscopic magnetization is obtained by calculating the definite integral of the $S(T)$ function.^{23,28} This is experimentally demonstrated by Figures 3 and 4 and also by overlapping of M_0 with M_{TRM} .

C. Slow dynamics and $M(H)$ irreversibility

Further indicative qualitative and quantitative differences in the magnetic behavior of the three compounds can be obtained from the magnetic hysteresis $M(H)$ loops measured

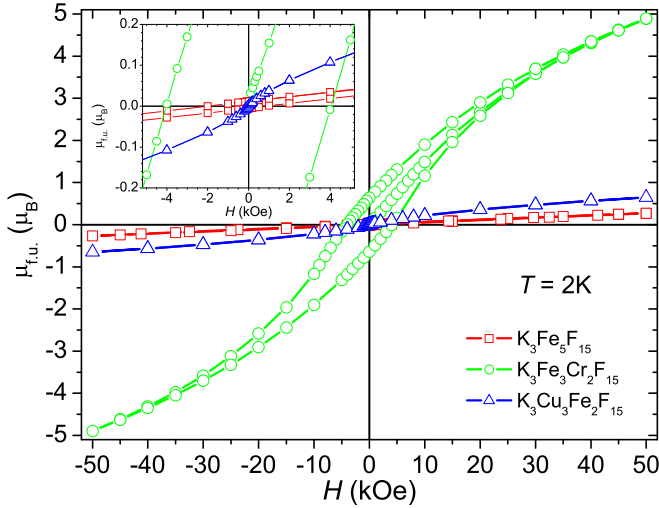


FIG. 5. Magnetic hysteresis loops measured at a temperature of 2 K. Inset: Enlarged low field region.

at 2 K shown in Fig. 5. The shape of $M(H)$ loop of $K_3Fe_5F_{15}$ and the absence of saturation, as well as its small magnetic moment of around $0.2 \mu_B$ (Bohr magnetons) per formula unit at 50 kOe indicate antiferromagnetic interactions modified with weak ferromagnetism. The hysteresis loops retain their shape up to T_N , with gradual decrease of remanent magnetization M_r and coercive field H_c . Above T_N , the $M(H)$ curves become linear in fields up to 50 kOe with almost the same slope as below T_N .¹⁶ Together with high irreversibility field H_{irr} , above which the two branches of the $M(H)$ loop overlap (near to 50 kOe at 2 K), this points to the coexistence of magnetic regions with large anisotropy and global antiferromagnetism. H_{irr} decreases with increase of temperature, but is still relatively high and much higher than in the other two compounds.¹⁶ Completely different behavior appears in $K_3Fe_3Cr_2F_{15}$, where the magnetization attains $5 \mu_B$ per formula unit in a 50 kOe field and there is bending toward saturation (although still far away). The hysteresis loops become more and more narrow as the temperature increases. M_r and H_c decrease with increase of temperature and vanish above 40 K.¹⁷ The $M(H)$ behavior of $K_3Fe_3Cr_2F_{15}$, as well as $M_r(T)$ and $H_c(T)$, is very reminiscent of the generic behavior of blocked superparamagnetic systems.^{23,25,27–29} On the other hand, $K_3Cu_3Fe_2F_{15}$ has a much narrower magnetic hysteresis which disappears above 4–5 K. The linear high field region is characteristic of a paramagnetic response, whereas the well observable bending of the magnetization at relatively small field (insets of Fig. 5) might originate in the greater magnetic moments of the ordered regions. These two magnetic components in $K_3Cu_3Fe_2F_{15}$ were envisaged in magnetic resonance experiments.²¹

All these facts allow us to connect the hysteretic irreversibility with the blocking and activation of the finite magnetic regions.

D. Magnetic nano-regions and their importance for multiferroic coupling

From the parameters obtained during analysis of the measurements and taking into account the two type magnetic

moment model of relaxation, we will estimate roughly the characteristic size of the relaxing magnetic regions. The barrier height U which blocks the magnetic unit against reorientation is related to the anisotropy energy density K and the volume of the relaxing unit V . To a first approximation, the relation $U = K \cdot V$ may be assumed, neglecting the shape and boundary effects on the anisotropy energy. The characteristic barrier height can be obtained from the macroscopic magnetization measurements. For relaxation of superparamagnetic systems, splitting between the ZFC and FC magnetization curves occurs below the blocking temperature T_B where the fluctuations of magnetic moments are slower than the experimental time, $\tau_{exp.} \approx 10$ s, needed for a single measurement.^{23,25} Usually, from the relaxation time τ given by the Arrhenius law $\tau = \tau_0 \exp(U/k_B T)$, where $1/\tau_0$ is the attempt frequency of the order such that $\tau_0 = 10^{-10}$ s, since the reorientation of the whole magnetic nano-region is considered.²³ Taking $\tau = \tau_{exp.}$, a relation $U \approx 25k_B T_B$ would be obtained. However, the two component origin of the shapes of the ZFC-FC and M_{TRM} curves makes the determination of T_B inappropriate. Instead, the temperatures T_{Smax} where the maxima of $S(T)$ appear are more appropriate for determination of the characteristic energy barriers. In that case, the above prefactor should be corrected to include the longer time of relaxation measurement (one hour) compared with the ZFC-FC $M(t)$ measurements. Therefore, $U \approx 30k_B T_{Smax}$ is more suitable here. The maxima T_{Smax} are taken from the lowest field measurements in order to avoid magnetic field distortion of the barriers.

The anisotropy density K is derivable from the macroscopic magnetic hysteresis loop measurement. The usual Stoner-Wohlfarth theoretical approach gives $K = H_c M_s / 2$, but this should be modified in our case, because saturation determination would be questionable and uncertain. To a good approximation, the anisotropy density could be determined from the irreversibility point on the hysteresis loop, (H_{irr}, M_{irr}) where the two branches of the $M(H)$ loop meet, as was applied for the Gd-Tb-Cu system.²⁷ Considering the anisotropy role in energy relations, the expression $K_{eff} = H_{irr} M_{irr}$ could be used to approximate the effective anisotropy energy density K_{eff} , where M_{irr} should be normalized to the volume magnetization, using the mass densities 3.5 g cm^{-3} , 3.4 g cm^{-3} , and 3.6 g cm^{-3} , for $K_3Fe_5F_{15}$, $K_3Fe_3Cr_2F_{15}$, and $K_3Cu_3Fe_2F_{15}$, respectively. The lowest possible temperature measurements (2 K) should be used in order to neglect thermal effects. The diameter of the relaxing magnetic regions is obtained as $d = (6V/\pi)^{1/3}$. d represents the characteristic effective size only, since the distribution details are not taken into account. The calculated values are shown in Table I.

The dimensions of the magnetic nano-regions obtained are rough estimates only, because of the many approximations used. However, the results show that the magnetically relaxing regions are of nano-sized. These magnetic regions are nano-sized and are in general agreement with the shapes of the $M(H)$ curves. For example, the curvature of $M(H)$ indicates larger magnetic nano-regions in $K_3Cu_3Fe_2F_{15}$ than in $K_3Fe_5F_{15}$, in accordance with the results in Table I. The region sizes in $K_3Cu_3Fe_2F_{15}$ determined by the two mentioned methods (from $H_{irr} \cdot M_{irr}$ and from $H_c \cdot M_s / 2$) are in

TABLE I. Parameters (with relevant standard deviations) important for determination of magnetic region size: peak position in logarithmic relaxation rate T_{Smax} , effective barrier height U , irreversibility field H_{irr} , corresponding irreversibility magnetization M_{irr} , effective anisotropy energy density K_{eff} , and magnetic region diameter d calculated for two values of T_{Smax} where applicable.

compound	$T_{Smax}(K)$	$U(J)$	$H_{irr}(Oe)$	$M_{irr}(emu/g)$	$K_{eff}(Jm^{-3})$	$d(nm)$
$K_3Fe_5F_{15}$	90 ± 2	3.7×10^{-20}	$50\,000 \pm 5000$	2.2 ± 0.4	$(39 \pm 08) \times 10^4$	12 ± 1
$K_3Fe_3Cr_2F_{15}$	10 ± 1	4.1×10^{-21}	$40\,000 \pm 4000$	36 ± 1	$(55 \pm 05) \times 10^5$	2.5 ± 0.2
	30 ± 3	1.2×10^{-20}				3.6 ± 0.3
$K_3Cu_3Fe_2F_{15}$	3 ± 0.3	1.2×10^{-21}	800 ± 100	0.25 ± 0.03	$(7 \pm 1) \times 10^1$	32 ± 2
	15 ± 3	6.2×10^{-21}				55 ± 5

agreement. This points to well defined magnetic regions, as was suggested from the NMR and EPR experiments.²¹ In $K_3Fe_3Cr_2F_{15}$, the two methods also give approximately the same sizes. In $K_3Fe_5F_{15}$, we can analyze only the peak at 90 K, and the peak at 120 K cannot be considered since it is very near to the phase transition.

Recently, muon spin relaxation experiments revealed the two component nature of magnetic organization in the same three compounds.³⁴ Using a completely different technique from ours, the short range magnetic order of the nano-regions was also revealed.

The nanometer scale magnetic order exhibited in $K_3M_3^{II}M_2^{III}F_{15}$ points to the perspectives of multiferroicity research in these systems, especially to the magneto-electric coupling for which polar and/or magnetic inhomogeneity on the nano-scale is important.^{35,36} The presence of magnetic nano-regions enhances the spiraling of the magnetic moments, especially on the boundaries of the regions, which breaks the local spatial symmetry and allows the onset of polarization. This kind of coupling was suggested recently in another system with multiferroic nano-regions.³⁵ Magnetic inhomogeneities on nanometer scale influences drastically the local polarizability and conductivity,³⁶ with positive implications for the application of multiferroics and understanding the nature of magneto-electric coupling. Further, importance of the magnetic anisotropy in the electric field induced magnetic domain formation was recently found experimentally.³⁷

V. CONCLUSIONS

A comparative study of the ZFC-FC magnetization curves and magnetic hysteresis loops in the $K_3M_3^{II}M_2^{III}F_{15}$ systems showed diverse magnetic behavior, including the moment blocking phenomena and magnetic irreversibility.

Slow magnetic dynamics observed in the three investigated multiferroic compounds throws new light on previously published work about their magnetic ordering.

The logarithmic time relaxation of magnetization over a broad range of temperatures and magnetic fields indicated a broad distribution of magnetic moments over the blocking anisotropy energy barriers in each of the $K_3M_3^{II}M_2^{III}F_{15}$ compounds.

All the experiments performed show in all three compounds the existence of two groups of moments. In the $S(T)$ dependence, the existence of two groups of energy barriers is expressed by two maxima, whereas in the $M_0(T)$, $M_{TRM}(T)$, and ZFC-FC $M(T)$ curves two groups of moments are

expressed through occurrence of the two steep descents separated by plateaus.

The correspondence between the ZFC-FC $M(T)$ curves, logarithmic relaxation rate $S(T)$, starting magnetization $M_0(T)$, and the thermoremanent magnetization $M_{TRM}(T)$ confirms the validity of the model of thermal activation of magnetic moments leading to the observed slow magnetic relaxation. The interplay of magnetic field and temperature in the behavior of these quantities indicates competition/cooperation of field and temperature in the activation of magnetic moments.

Our investigation of relaxation confirmed the formation of magnetic nano-regions in $K_3M_3^{II}M_2^{III}F_{15}$ systems and gave the size of these nano-regions for all three fluorides, which is in accordance with recent findings from different experiments. The obtained results on nanometer-sized anisotropic magnetic regions have some relevance for the magneto-electric coupling in $K_3M_3^{II}M_2^{III}F_{15}$ compounds.

ACKNOWLEDGMENTS

Our sincere thanks goes to the deceased colleague Professor Robert Blinc who was deeply involved in the early investigations of fluoride multiferroics and pointed to us this topic. We were grateful to Boris Žemva, Gašper Tavčar, and Evgenij Goreschnik from the Jožef Stefan Institute, Ljubljana, for synthesis, XRD measurements, and analysis of the samples. This research was supported by the Slovene Research Agency (Program P2-0348). The work of D.P. was financially supported by the Slovene Human Resources and Scholarship Fund within the Ad Futura Programme and the National Foundation for Science, Higher Education and Technological Development of the Republic of Croatia within the Brain Gain Programme.

¹J. Kreisel and M. Kenzelmann, *Europhys. News* **40/5**, 17 (2009).

²N. A. Spaldin and M. Fiebig, *Science* **309**, 391 (2005).

³K. F. Wang, J.-M. Liu, and Z. F. Ren, *Adv. Phys.* **58**, 321 (2009).

⁴G. Catalan and J. F. Scott, *Adv. Mater.* **21**, 2463 (2009).

⁵J. F. Scott, *Science* **315**, 954 (2007).

⁶H. Béa, M. Gajek, M. Bibes, and A. Barthélémy, *J. Phys.: Condens. Matter* **20**, 434221 (2008).

⁷M. Gajek, M. Bibes, S. Fusil, K. Bouzehouane, J. Fontcuberta, A. Barthélémy, and A. Fert, *Nature Mater.* **6**, 296 (2007).

⁸A. K. Zvezdin, A. S. Logginov, G. A. Meshkov, and A. P. Pyatakov, *Bull. Russ. Acad. Sci.: Phys.* **71**, 1561 (2007).

⁹M. Josse, O. Bidault, F. Roulland, E. Castel, A. Simon, D. Michau, R. Von der Mühl, O. Nguyen, and M. Maglione, *Solid State Sci* **11**, 1118 (2009).

¹⁰G. Nénert and T. T. M. Palstra, *J. Phys.: Condens. Matter* **19**, 406213 (2007).

¹¹S. Fabbri, E. Montanari, L. Righi, G. Calestani, and A. Migliori, *Chem. Mater.* **16**, 3007 (2004).

- ¹²N. A. Hill, *J. Phys. Chem.* **104**, 6694 (2000).
- ¹³J. F. Scott, R. Palai, A. Kumar, M. K. Singh, N. M. Murari, N. K. Karan, and R. S. Katiyar, *J. Am. Ceram. Soc.* **91**, 1762 (2008).
- ¹⁴J. Ravez, S. C. Abrahams, and R. de Pape, *J. Appl. Phys.* **65**, 3987 (1989).
- ¹⁵S. Ishihara, J.-P. Rivera, E. Kita, Z.-G. Ye, F. Kubel, and H. Schmid, *Ferroelectrics* **162**, 51 (1994).
- ¹⁶R. Blinc, G. Tavčar, B. Žemva, D. Hanžel, P. Cevc, C. Filipič, A. Levstik, Z. Jagličić, Z. Trontelj, and N. Dalal, *J. Appl. Phys.* **103**, 074114 (2008).
- ¹⁷R. Blinc, P. Cevc, A. Potočnik, B. Žemva, E. Goresnik, D. Hanžel, A. Gregorovič, Z. Trontelj, Z. Jagličić, V. Laguta, M. Perović, N. S. Dalal, and J. F. Scott, *J. Appl. Phys.* **107**, 043511 (2010).
- ¹⁸R. Blinc, G. Tavčar, B. Žemva, E. Goresnik, D. Hanžel, P. Cevc, A. Potočnik, V. Laguta, Z. Trontelj, Z. Jagličić, and J. F. Scott, *J. Appl. Phys.* **106**, 023924 (2009).
- ¹⁹A.-M. Hardy, A. Hardy, and G. Ferey, *Acta Crystallogr., Sect. B: Struct. Crystallogr. Cryst. Chem.* **29**, 1654 (1973).
- ²⁰F. Mezzadri, S. Fabbri, E. Montanari, L. Righi, G. Calestani, E. Gilioli, F. Bolzoni, and A. Migliori, *Phys. Rev. B* **78**, 064111 (2008).
- ²¹R. Blinc, B. Zalar, P. Cevc, A. Gregorovič, B. Žemva, G. Tavčar, V. Laguta, J. F. Scott, and N. Dalal, *J. Phys.: Condens. Matter* **21**, 045902 (2009).
- ²²The temperature dependence of XRD in Cr and Cu compound is not yet known.
- ²³E. M. Chudnovsky and J. Tejada, *Macroscopic Quantum Tunneling of the Magnetic Moment* (Cambridge University Press, Cambridge, UK, 1998).
- ²⁴F. Mezzadri, G. Calestani, C. Pernechele, M. Solzi, G. Spina, L. Ciani, F. Del Giallo, M. Lantieri, M. Buzzi, and E. Gilioli, *Phys. Rev. B* **84**, 104418 (2011).
- ²⁵T. G. St. Pierre, N. T. Gorham, P. D. Allen, J. L. Costa-Krämer, and K. V. Rao, *Phys. Rev. B* **65**, 024436 (2001).
- ²⁶D. Pajić, K. Zadro, R. E. Vandenberghe, and I. Nedkov, *J. Magn. Magn. Mater.* **281**, 353 (2004).
- ²⁷J. I. Arnaudas, A. del Moral, C. de la Fuente, and P. A. J. de Groot, *Phys. Rev. B* **47**, 11924 (1993).
- ²⁸D. Pajić, K. Zadro, R. Ristić, I. Živković, Ž. Skoko, and E. Babić, *J. Phys.: Condens. Matter* **19**, 296207 (2007).
- ²⁹J. Tejada, R. F. Ziolo, and X. X. Zhang, *Chem. Mater.* **8**, 1784 (1996).
- ³⁰W. Götze and M. Sperl, *Phys. Rev. E* **66**, 011405 (2002).
- ³¹D. Chowdhury and A. Mookerjee, *J. Phys. F: Met. Phys.* **14**, 245 (1984).
- ³²V. Skumryev, F. Ott, J. M. D. Coey, A. Anane, J.-P. Renard, L. Pinsard-Gaudart, and A. Revcolevschi, *Eur. Phys. J. B* **11**, 401 (1999).
- ³³Z. Jagličić, private communication (2009).
- ³⁴A. Potočnik, A. Zorko, D. Arčon, E. Goresnik, B. Žemva, R. Blinc, P. Cevc, Z. Trontelj, Z. Jagličić, and J. F. Scott, *Phys. Rev. B* **81**, 214420 (2010).
- ³⁵W. B. Wu, D. J. Huang, J. Okamoto, S. W. Huang, Y. Sekio, T. Kimura, and C. T. Chen, *Phys. Rev. B* **81**, 172409 (2010).
- ³⁶J. Seidel, L. W. Martin, Q. He, Q. Zhan, Y.-H. Chu, A. Rother, M. E. Hawkrige, P. Maksymovych, P. Yu, M. Gajek, N. Balke, S. V. Kalinin, S. Gemming, F. Wang, G. Catalan, J. F. Scott, N. A. Spaldin, J. Orenstein, and R. Ramesh, *Nature Mater.* **8**, 229 (2009).
- ³⁷T. H. E. Lahtinen, J. O. Tuomi, and S. van Dijken, *Adv. Mater.* **23**, 3187 (2011).